Science Advances
AAAS

Supplementary Materials for

Single-cell multiomics sequencing reveals the reprogramming defects in embryos generated by round spermatid injection

Jing Wang *et al.*

Corresponding author: Lin Li, lilin2019@i.smu.edu.cn, Gang Chang, changgang@szu.edu.cn, Xiao-Yang Zhao, zhaoxiaoyang@smu.edu.cn.

Sci. Adv. **8**, eabm3976 (2022)
DOI: 10.1126/sciadv.abm3976

The PDF file includes:

Figs. S1 to S14
Legends for tables S1 to S7

Other Supplementary Material for this manuscript includes the following:

Tables S1 to S7

Supplementary Tables:

Table S1. The developmental potential of pre-implantation and post-implantation mouse embryos.

Table S2. Basic summary of single-cell multi-omics sequencing data in each individual cell that passed quality control.

Table S3. DEGs between ICSI and ROSI embryos at different stages.

Table S4. DEGs associated with NDRs and DEGs associated with DMRs.

Table S5. DEGs, NDRs, and DMRs amended by A366 treatment.

Table S6. List of some small compounds related to epigenetic modifications.

Table S7. Target sequences of siRNA, the primers for qPCR, liDNaseI-qPCR, bisulfite genomic PCR, and cDNA-cloning.

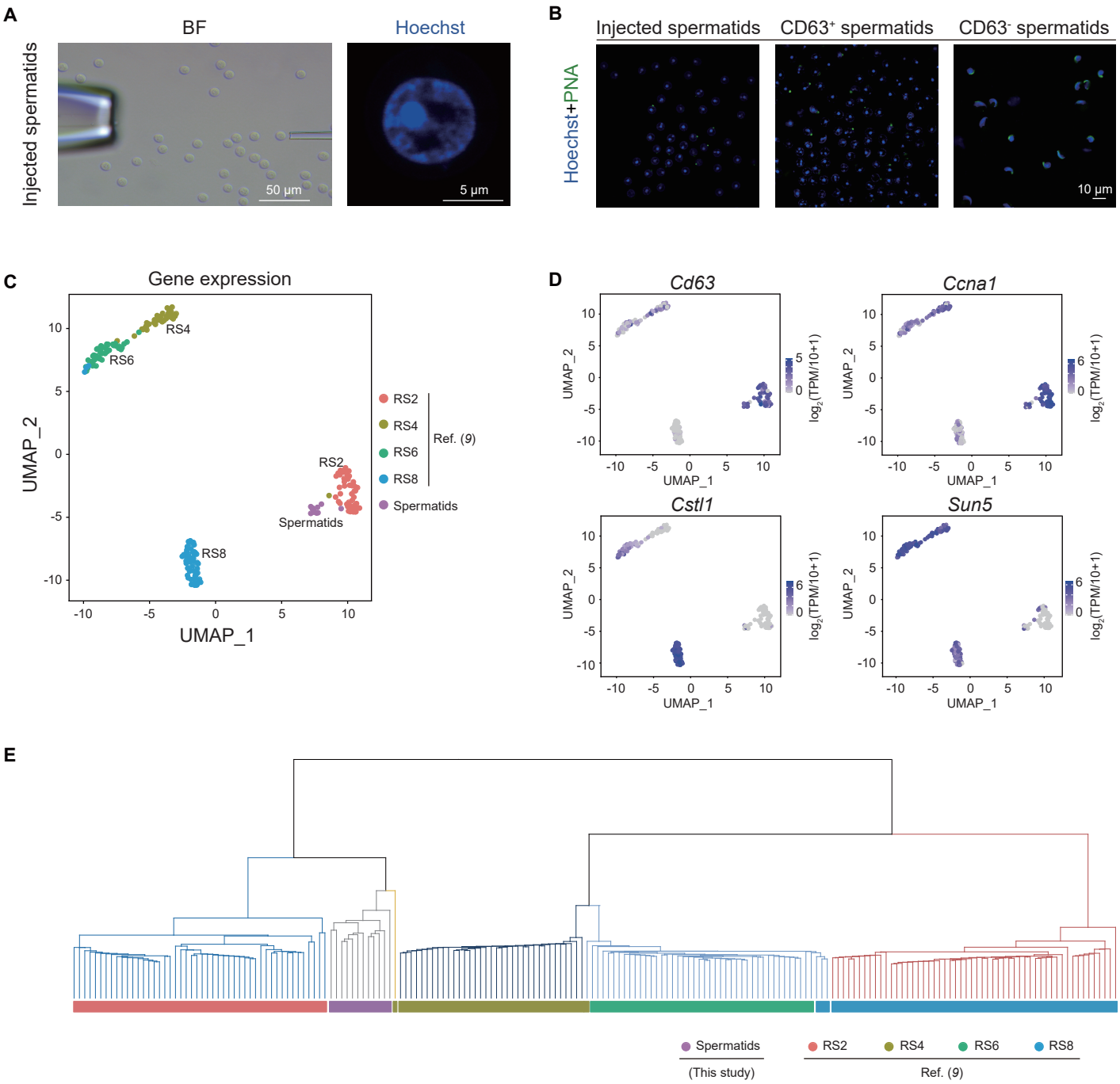
A
BF
Hoechst
Injected spermatids
50 μm
5 μm
B
Injected spermatids
CD63+ spermatids
CD63- spermatids
Hoechst+PNA
10 μm
C
Gene expression
RS4
RS6
RS2
Spermatids
RS8
UMAP_2
UMAP_1
RS2
RS4
RS6
RS8
Spermatids
Ref. (9)
D
Cd63
Ccna1
Cstl1
Sun5
UMAP_2
UMAP_1
log2(TPM/10+1)
E
Spermatids
(This study)
RS2
RS4
RS6
RS8
Ref. (9)

Figure S1. Characterization of the early-stage round spermatids used in this study.

(**A**) Representative images showing the morphology of round spermatids used in this study (left). Hoechst 33342 staining showing a representative round spermatid with a centrally located chromatin granule within the nucleus (right).

(**B**) Immunofluorescence of PNA in round spermatids used in this study (left), and the early-stage round spermatids ($CD63^+$, middle) as well as late-stage round spermatids ($CD63^-$, right) sorted by FACS as previously described (*9*).

(**C**) UMAP plot showing transcriptome data of round spermatids used in this study (n = 12) by integrating with the datasets of different stages of round spermatids in a previous study (*9*) (n = 184). Cells are colored by stage and experimental group.

(**D**) UMAP plots showing the expression levels of marker genes in the round spermatids at different developmental stages. The color from gray to blue indicates low to high expression levels.

(**E**) K-means clustering of round spermatids used in this study and different stages of round spermatids in a previous study (*9*) based on the gene expression data.

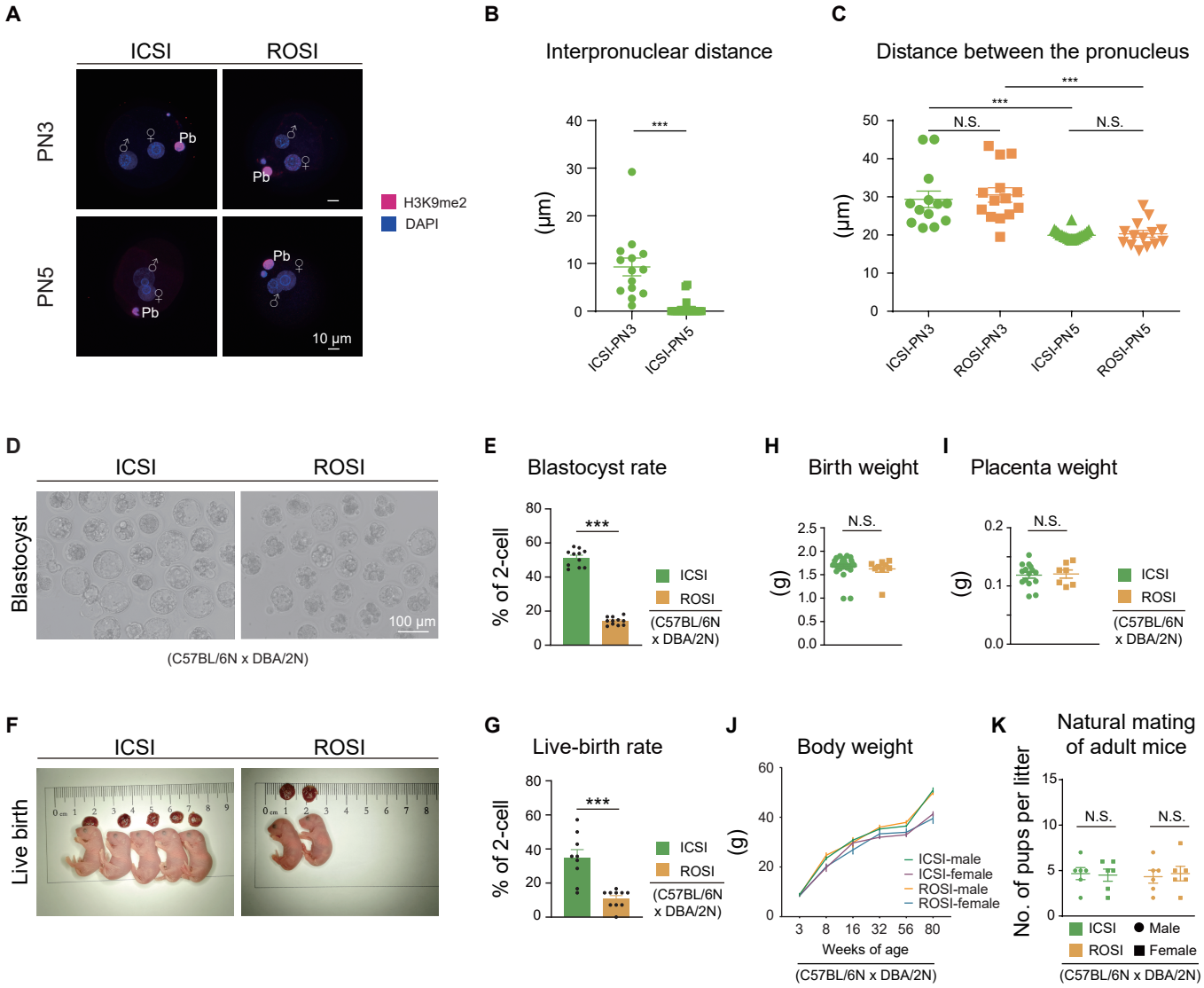
A
ICSI
ROSI
PN3
PN5
Pb
H3K9me2
DAPI
10 μm
B
Interpronuclear distance
(μm)
***
ICSI-PN3
ICSI-PN5
C
Distance between the pronucleus
N.S.
ROSI-PN3
ROSI-PN5
D
Blastocyst
100 μm
(C57BL/6N x DBA/2N)
E
Blastocyst rate
% of 2-cell
F
Live birth
G
Live-birth rate
H
Birth weight
(g)
I
Placenta weight
J
Body weight
ICSI-male
ICSI-female
ROSI-male
ROSI-female
Weeks of age
K
Natural mating of adult mice
No. of pups per litter
Male
Female

Figure S2. The developmental progress of pronuclear stage embryos derived by ICSI and ROSI at 7.5 h and 12 h post-injection, and the developmental potential of ROSI embryos.

(**A**) Representative immunofluorescence images of embryos at the pronuclear stages derived by ICSI and ROSI at 7.5 h (PN3) and 12 h (PN5) post-injection. Embryos are fixed and permeabilized using 4% paraformaldehyde containing 0.2% Triton X-100 for 20 min at room temperature. Blue: DAPI, red: H3K9me2. Pb: polar body, ♀: female pronucleus, ♂: male pronucleus. Scale bars, 10 μm.

(**B**) Dot plot showing the interpronuclear distance of embryos at the pronuclear stages derived by ICSI at 7.5 h (PN3, n = 14) and 12 h (PN5, n = 20) post-injection. ***$P < 0.001$, unpaired two-tailed Student's *t* test.

(**C**) Dot plot showing the geometric center distance between two pronuclei of embryos at the pronuclear stages derived by ICSI (PN3, n = 13; PN5, n = 20) and ROSI (PN3, n = 14; PN5, n = 14) in three biological replicates. ***$P < 0.001$, N.S., not significant, unpaired two-tailed Student's *t* test.

(**D**) Representative ROSI and ICSI blastocysts at 94 h post-injection. Scale bar, 100 μm.

(**E**) Blastocyst rate of ROSI and ICSI embryos in eleven biological replicates. ***$P < 0.001$, unpaired two-tailed Student's *t* test.

(**F**) Representative alive fetuses produced from ROSI and ICSI groups at E19.5.

(**G**) Live-birth rate of ROSI and ICSI embryos. ***$P < 0.001$, unpaired two-tailed Student's *t* test. Nine (ICSI) and ten (ROSI) replicates are performed.

(**H**) Dot plot showing the birth weight (ICSI, n = 26; ROSI, n = 7) of alive fetuses from ROSI and ICSI groups in five biological replicates. N.S., not significant, unpaired two-tailed Student's *t* test.

(**I**) Dot plot showing the placenta weight (ICSI, n = 15; ROSI, n = 7) of alive fetuses from ROSI and ICSI groups in five biological replicates. N.S., not significant, unpaired two-tailed Student's *t* test.

(**J**) Line chart showing the body weight of mice (from 3 to 80 week) from ROSI and ICSI groups. n = 3 per group.

(**K**) Dot plot showing the litter size of natural mating of adult mice from ROSI and ICSI groups in six biological replicates. N.S., not significant, unpaired two-tailed Student's *t* test.

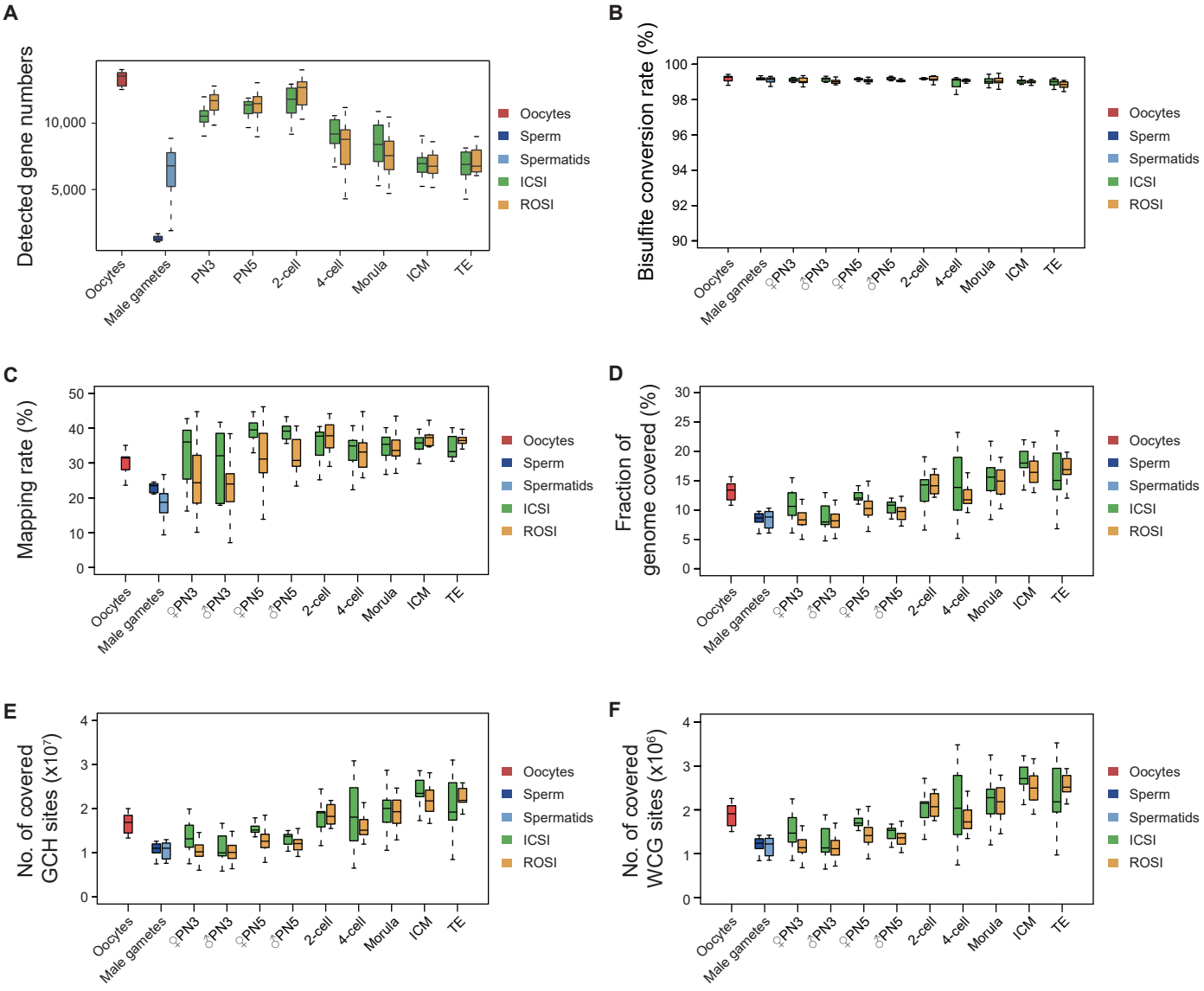
A
Detected gene numbers
10,000
5,000
Oocytes
Male gametes
PN3
PN5
2-cell
4-cell
Morula
ICM
TE
Oocytes
Sperm
Spermatids
ICSI
ROSI
B
Bisulfite conversion rate (%)
100
98
96
94
92
90
Oocytes
Male gametes
♀PN3
♂PN3
♀PN5
♂PN5
2-cell
4-cell
Morula
ICM
TE
Oocytes
Sperm
Spermatids
ICSI
ROSI
C
Mapping rate (%)
50
40
30
20
10
0
Oocytes
Male gametes
♀PN3
♂PN3
♀PN5
♂PN5
2-cell
4-cell
Morula
ICM
TE
Oocytes
Sperm
Spermatids
ICSI
ROSI
D
Fraction of genome covered (%)
30
25
20
15
10
5
0
Oocytes
Male gametes
♀PN3
♂PN3
♀PN5
♂PN5
2-cell
4-cell
Morula
ICM
TE
Oocytes
Sperm
Spermatids
ICSI
ROSI
E
No. of covered GCH sites (X10⁷)
4
3
2
1
0
Oocytes
Male gametes
♀PN3
♂PN3
♀PN5
♂PN5
2-cell
4-cell
Morula
ICM
TE
Oocytes
Sperm
Spermatids
ICSI
ROSI
F
No. of covered WCG sites (x10⁶)
4
3
2
1
0
Oocytes
Male gametes
♀PN3
♂PN3
♀PN5
♂PN5
2-cell
4-cell
Morula
ICM
TE
Oocytes
Sperm
Spermatids
ICSI
ROSI

Figure S3. Quality control of single-cell multi-omics sequencing datasets.

(**A**) Boxplot showing the gene number detected in each individual cell.

(**B-D**) Boxplots showing the bisulfite conversion rate (B), mapping rate (C), and genome coverage (D) of DNA part data in each individual cell.

(**E-F**) Boxplots showing the numbers of GCH (GCA/GCT/GCC) sites (E) and WCG (ACG/TCG) sites (F) covered at 1× depth of DNA part data in each individual cell.

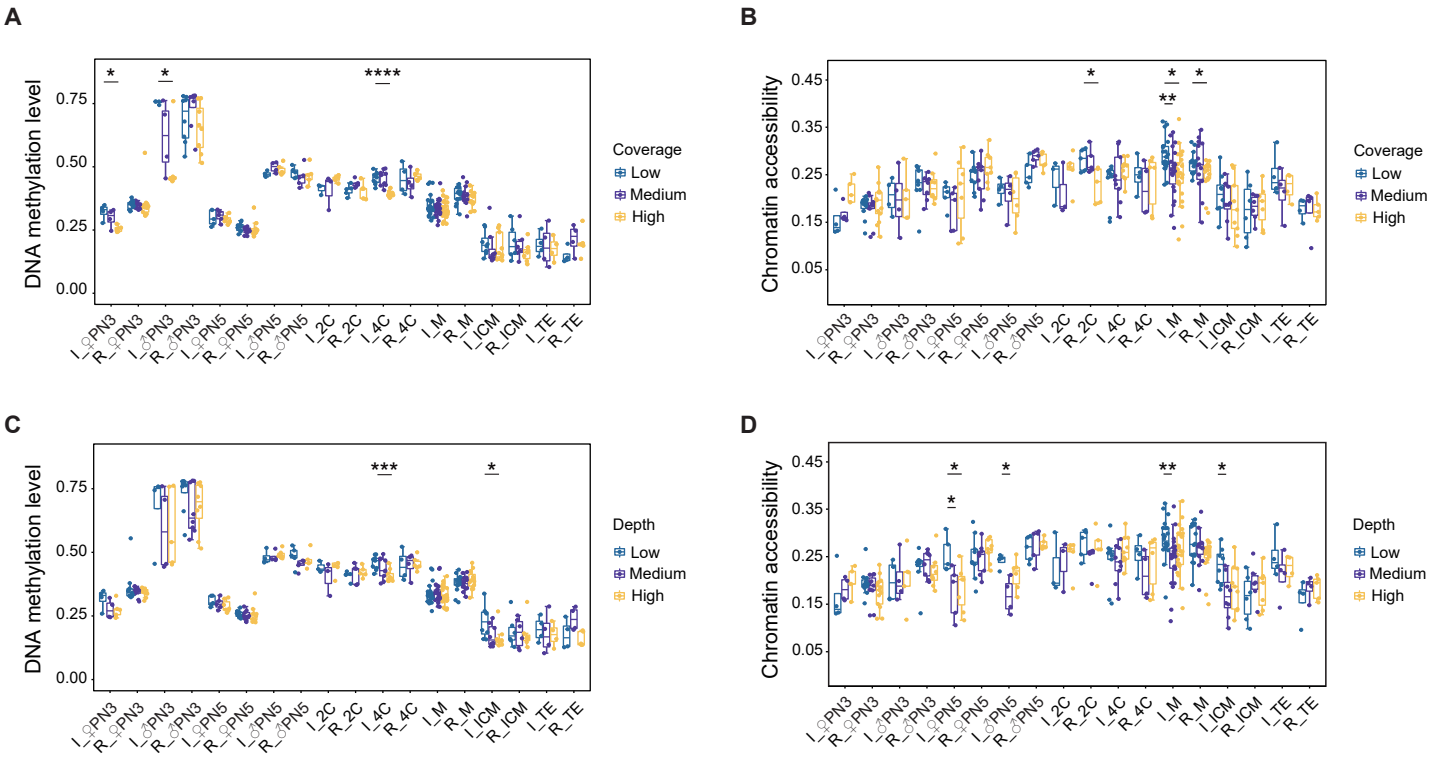
A
DNA methylation level
0.00
0.25
0.50
0.75
*
*
****
Coverage
Low
Medium
High
B
Chromatin accessibility
0.05
0.15
0.25
0.35
0.45
*
*
**
*
Coverage
Low
Medium
High
C
DNA methylation level
0.00
0.25
0.50
0.75
***
*
Depth
Low
Medium
High
D
Chromatin accessibility
0.05
0.15
0.25
0.35
0.45
*
*
*
**
*
Depth
Low
Medium
High
I_♀PN3
R_♀PN3
I_♂PN3
R_♂PN3
I_♀PN5
R_♀PN5
I_♂PN5
R_♂PN5
I_2C
R_2C
I_4C
R_4C
I_M
R_M
I_ICM
R_ICM
I_TE
R_TE

Figure S4. **The dynamics of chromatin accessibility and DNA methylation are mainly consistent in groups with different coverage or depth.**

(**A-B**) Boxplots showing the DNA methylation level (A) and chromatin accessibility (B) of each individual cell with low (blue), medium (purple), and high (yellow) genomic coverage.

(**C-D**) Boxplots showing the DNA methylation level (C) and chromatin accessibility (D) of each individual cell with low (blue), medium (purple), and high (yellow) sequencing depth.

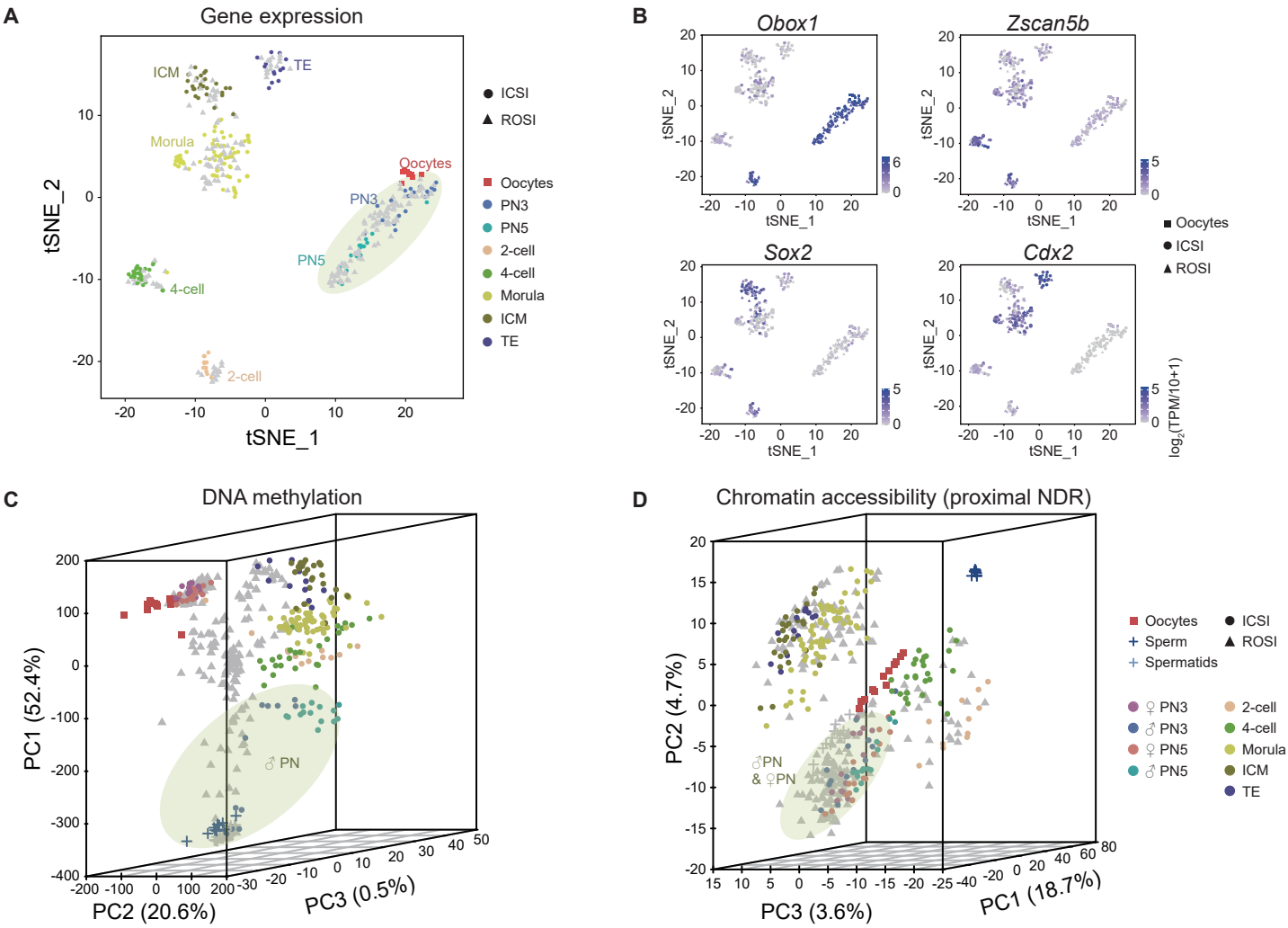
A
Gene expression
ICM
TE
Morula
Oocytes
PN3
PN5
4-cell
2-cell
tSNE_1
tSNE_2
ICSI
ROSI
Oocytes
PN3
PN5
2-cell
4-cell
Morula
ICM
TE
B
Obox1
Zscan5b
Sox2
Cdx2
tSNE_1
tSNE_2
log2(TPM/10+1)
Oocytes
ICSI
ROSI
C
DNA methylation
PC1 (52.4%)
PC2 (20.6%)
PC3 (0.5%)
♂ PN
D
Chromatin accessibility (proximal NDR)
PC2 (4.7%)
PC3 (3.6%)
PC1 (18.7%)
♂PN
& ♀PN
Oocytes
Sperm
Spermatids
ICSI
ROSI
♀ PN3
♂ PN3
♀ PN5
♂ PN5
2-cell
4-cell
Morula
ICM
TE

Figure S5. The dimensionality reduction analysis of transcriptome, chromatin accessibility, and DNA methylation data in the pre-implantation mouse embryos.

(**A**) Dimensionality reduction analysis of gene expression data using t-SNE. Each dot represents a single cell. ICSI samples are dots and are colored by the developmental stages, while ROSI samples are triangles and are in grey. Yellow-green circle indicates the pronuclei. (**B**) t-SNE plots showing the expression levels of marker genes, *Obox1* (oocyte and 1-cell), *Zscan5b* (2-cell), *Sox2* (ICM), *Cdx2* (TE). The color from gray to blue indicates low to high expression levels.

(**C-D**) Dimensionality reduction analysis of DNA methylation data in 500-bp windows (C) and chromatin accessibility in proximal NDRs (D) using PCA. Each dot represents a single cell. ICSI samples are dots and are colored by the developmental stages, while ROSI samples are triangles and are in grey. Yellow-green circle indicates male pronucleus (C), male and female pronuclei (D), respectively.

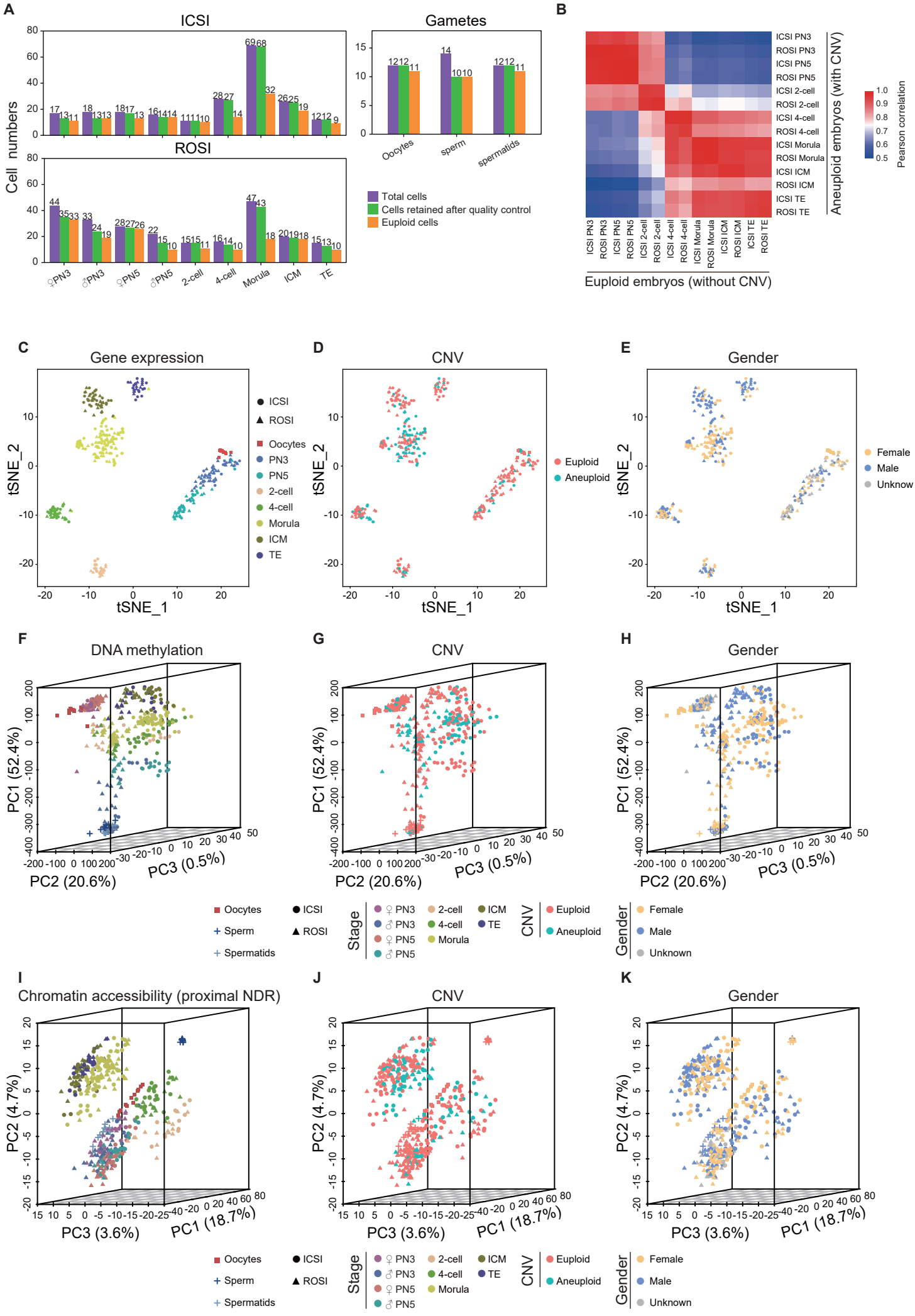
A
ICSI
ROSI
Cell numbers
♀PN3
♂PN3
♀PN5
♂PN5
2-cell
4-cell
Morula
ICM
TE
Gametes
Oocytes
sperm
spermatids
Total cells
Cells retained after quality control
Euploid cells
B
ICSI PN3
ROSI PN3
ICSI PN5
ROSI PN5
ICSI 2-cell
ROSI 2-cell
ICSI 4-cell
ROSI 4-cell
ICSI Morula
ROSI Morula
ICSI ICM
ROSI ICM
ICSI TE
ROSI TE
Aneuploid embryos (with CNV)
Pearson correlation
Euploid embryos (without CNV)
C
Gene expression
tSNE_1
tSNE_2
ICSI
ROSI
Oocytes
PN3
PN5
2-cell
4-cell
Morula
ICM
TE
D
CNV
Euploid
Aneuploid
E
Gender
Female
Male
Unknow
F
DNA methylation
PC1 (52.4%)
PC2 (20.6%)
PC3 (0.5%)
G
CNV
H
Gender
Oocytes
Sperm
Spermatids
ICSI
ROSI
Stage
♀PN3
♂PN3
♀PN5
♂PN5
2-cell
4-cell
Morula
ICM
TE
CNV
Euploid
Aneuploid
Gender
Female
Male
Unknown
I
Chromatin accessibility (proximal NDR)
PC2 (4.7%)
PC3 (3.6%)
PC1 (18.7%)
J
CNV
K
Gender

Figure S6. The overview of transcriptome, chromatin accessibility, and DNA methylation in euploid and aneuploid cells, and embryos with different gender derived by ICSI and ROSI.

(**A**) Bar plots showing the distributions of the number of total cells, cells retained after quality control, and euploid cells in ICSI (top), ROSI (bottom) as well as gametes (right) group, respectively.

(**B**) Heatmap showing the pearson correlation of transcriptome data between euploid and aneuploid cells from the pronuclear stage to blastocyst stage.

(**C-E**) Dimensionality reduction analysis of gene expression data colored by the developmental stages (C), CNVs (D), and gender information (E) using t-SNE. The dots represent the ICSI embryos and the triangles represent the ROSI embryos in fig. S6 C-E. The gray color in fig. S6E represents the embryos with unknown gender.

(**F-H**) Dimensionality reduction analysis of DNA methylation data in 500-bp windows colored by the developmental stages (F), CNVs (G), and gender information (H) using PCA. ROSI samples are triangles and ICSI samples are dots in fig. S6 F-H. The gray color in fig. S6H represents the embryos with unknown gender.

(**I-K**) Dimensionality reduction analysis of chromatin accessibility data colored by stage (I), CNVs (J), and gender information (K) using PCA. ROSI samples are triangles and ICSI samples are dots in fig. S6 I-K. The gray color in fig. S6K represents the embryos with unknown gender.

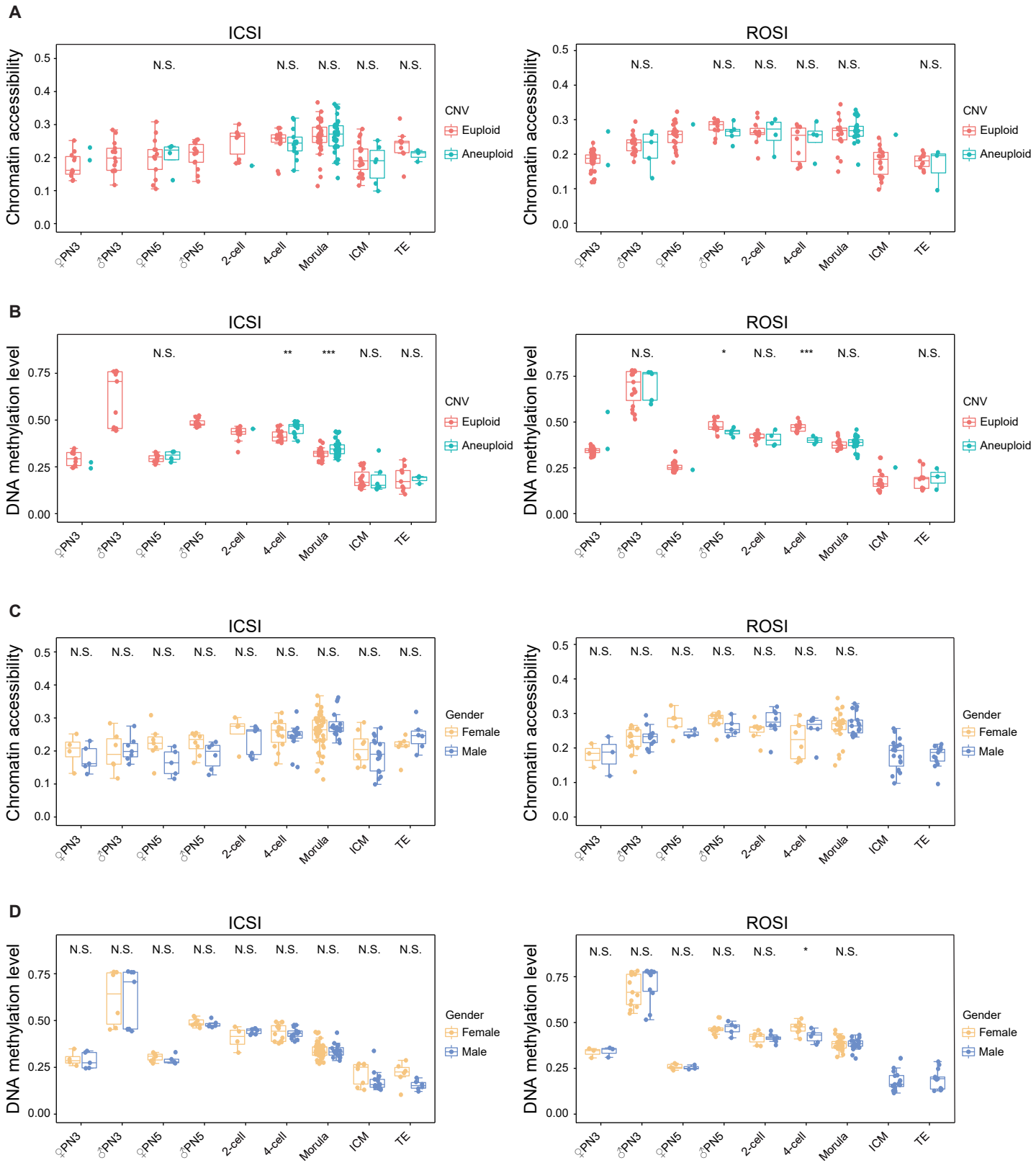
A
ICSI
ROSI
Chromatin accessibility
N.S.
CNV
Euploid
Aneuploid
♀PN3
♂PN3
♀PN5
♂PN5
2-cell
4-cell
Morula
ICM
TE
B
DNA methylation level
**
***
*
C
Gender
Female
Male
D

Figure S7. **The dynamics of chromatin accessibility and DNA methylation in euploid and aneuploid cells, and embryos with different gender derived by ICSI and ROSI.**

(**A**) Boxplots showing the chromatin accessibility in euploid and aneuploid cells in ICSI (left) and ROSI (right) embryos. N.S., not significant, unpaired two-tailed Student's *t* test.

(**B**) Boxplots showing the DNA methylation level in euploid and aneuploid cells in ICSI (left) and ROSI (right) embryos. **P* < 0.05, ***P* < 0.01, ****P* < 0.001, N.S., not significant, unpaired two-tailed Student's *t* test.

(**C**) Boxplots showing the chromatin accessibility in ICSI (left) and ROSI (right) embryos with different gender. N.S., not significant, unpaired two-tailed Student's *t* test.

(**D**) Boxplots showing the DNA methylation level in ICSI (left) and ROSI (right) embryos with different gender. **P* < 0.05, N.S., not significant, unpaired two-tailed Student's *t* test.

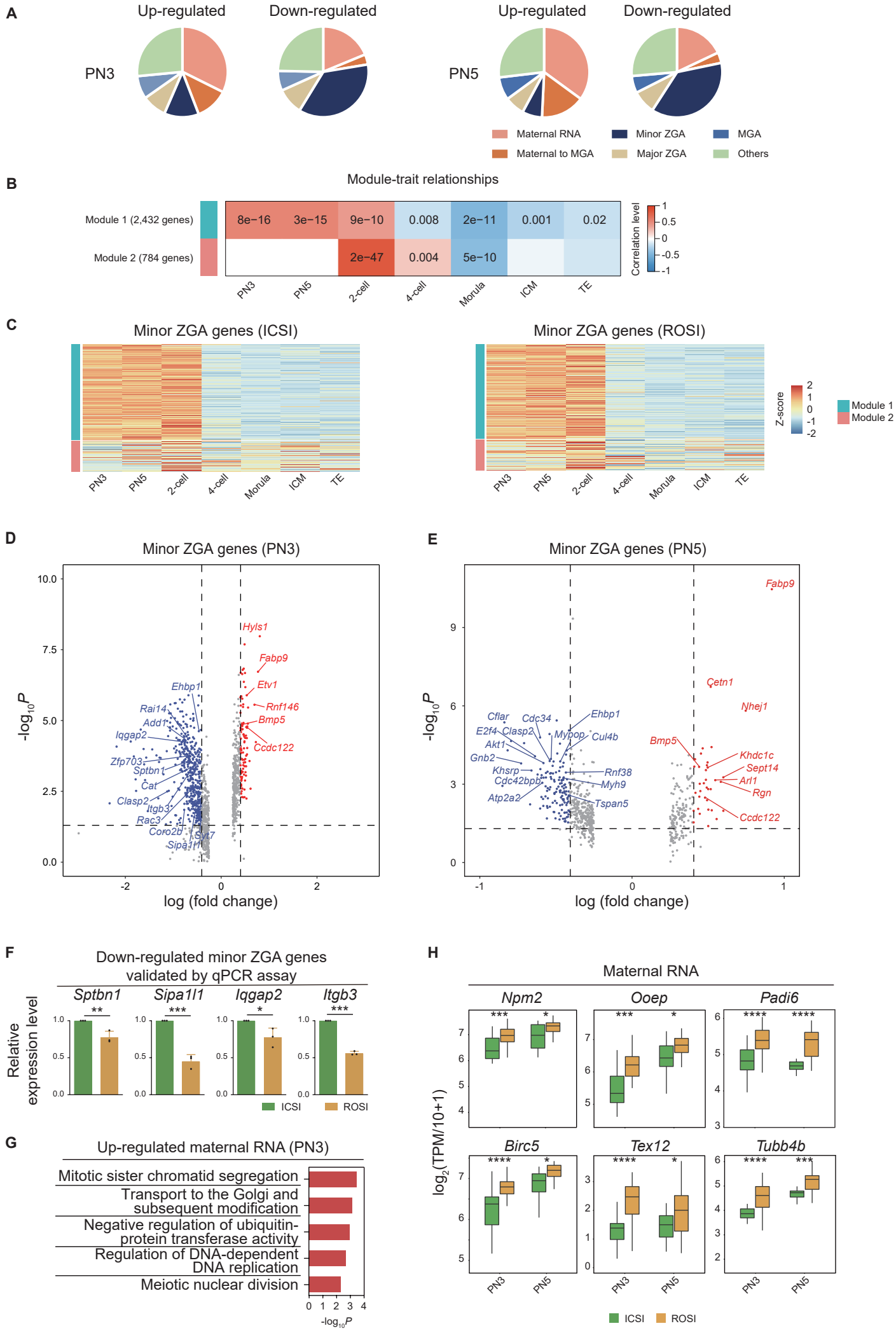
A
Up-regulated
Down-regulated
PN3
PN5
Maternal RNA
Maternal to MGA
Minor ZGA
Major ZGA
MGA
Others
B
Module-trait relationships
Module 1 (2,432 genes)
Module 2 (784 genes)
8e−16
3e−15
9e−10
0.008
2e−11
0.001
0.02
2e−47
0.004
5e−10
PN3
PN5
2-cell
4-cell
Morula
ICM
TE
Correlation level
C
Minor ZGA genes (ICSI)
Minor ZGA genes (ROSI)
Z-score
Module 1
Module 2
D
Minor ZGA genes (PN3)
-log10P
log (fold change)
Hyls1
Fabp9
Etv1
Rnf146
Bmp5
Ccdc122
Ehbp1
Rai14
Add1
Iqgap2
Zfp703
Sptbn1
Cat
Clasp2
Itgb3
Rac3
Coro2b
Syt7
Sipa1l1
E
Minor ZGA genes (PN5)
Fabp9
Çetn1
Nhej1
Bmp5
Khdc1c
Sept14
Arl1
Rgn
Ccdc122
Cflar
Cdc34
E2f4
Clasp2
Akt1
Gnb2
Khsrp
Cdc42bpb
Atp2a2
Ehbp1
Mypop
Cul4b
Rnf38
Myh9
Tspan5
F
Down-regulated minor ZGA genes validated by qPCR assay
Sptbn1
Sipa1l1
Iqgap2
Itgb3
Relative expression level
ICSI
ROSI
G
Up-regulated maternal RNA (PN3)
Mitotic sister chromatid segregation
Transport to the Golgi and subsequent modification
Negative regulation of ubiquitin-protein transferase activity
Regulation of DNA-dependent DNA replication
Meiotic nuclear division
-log10P
H
Maternal RNA
Npm2
Ooep
Padi6
Birc5
Tex12
Tubb4b
log2(TPM/10+1)
PN3
PN5
ICSI
ROSI

Figure S8. The mis-expression of maternal to zygotic transition associated genes in ROSI embryos.

(**A**) The proportion of each gene cluster in DEGs at the PN3 (left) and PN5 (right) stages.

(**B**) Heatmap showing the correlation between modules and different stages of minor ZGA genes. The number of genes in each module is marked on the left.

(**C**) Heatmaps showing the expression level of each module in ICSI (left) and ROSI (right) embryos.

(**D-E**) Volcano plots showing the differential gene expression of minor ZGA genes at the PN3 (D) and PN5 (E) stages. Up-regulated and down-regulated minor ZGA genes in ROSI embryos are shown as red dots and blue dots, respectively.

(**F**) Bar graphs showing the relative expression levels of 4 representative down-regulated minor ZGA genes at the PN3 stage validated by qPCR assay in three biological replicates. *$P < 0.05$, **$P < 0.01$, ***$P < 0.001$, unpaired two-tailed Student's *t* test.

(**G**) Enriched GO terms (powered by Metascape) of up-regulated maternal RNA genes in ROSI embryos (PN3). The x-axis represents the significance of relative GO terms ($-\log_{10}P$, hypergeometric testing).

(**H**) Expression levels ($\log_2$(TPM/10+1)) of up-regulated maternal RNA genes in ROSI and ICSI embryos at the PN3 and PN5 stages. *$P < 0.05$, ***$P < 0.001$, ****$P < 0.0001$, likelihood ratio test.

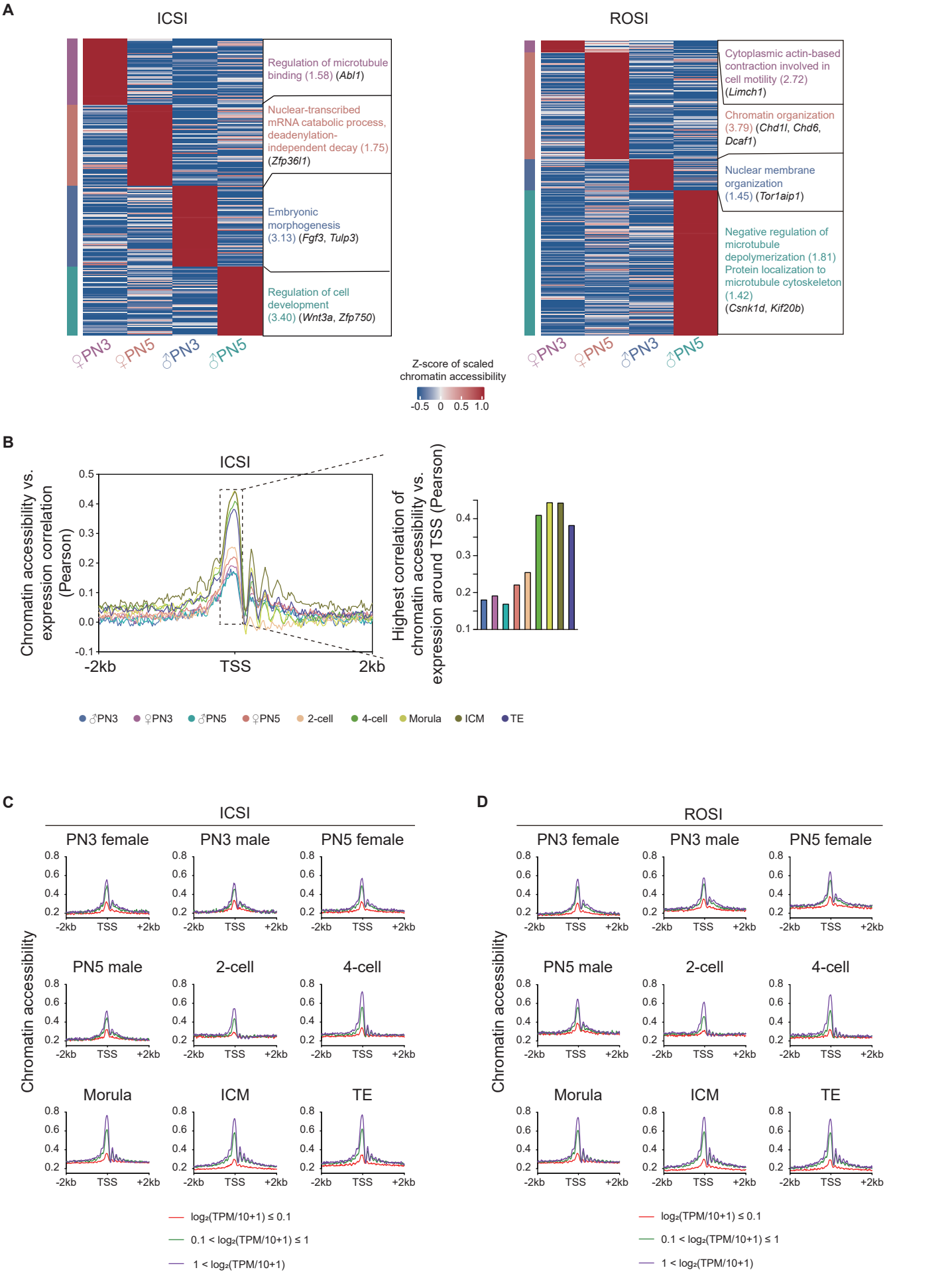
A
ICSI
ROSI
Regulation of microtubule binding (1.58) (Abl1)
Nuclear-transcribed mRNA catabolic process, deadenylation-independent decay (1.75) (Zfp36l1)
Embryonic morphogenesis (3.13) (Fgf3, Tulp3)
Regulation of cell development (3.40) (Wnt3a, Zfp750)
Cytoplasmic actin-based contraction involved in cell motility (2.72) (Limch1)
Chromatin organization (3.79) (Chd1l, Chd6, Dcaf1)
Nuclear membrane organization (1.45) (Tor1aip1)
Negative regulation of microtubule depolymerization (1.81)
Protein localization to microtubule cytoskeleton (1.42) (Csnk1d, Kif20b)
♀PN3 ♀PN5 ♂PN3 ♂PN5
Z-score of scaled chromatin accessibility
-0.5 0 0.5 1.0
B
ICSI
Chromatin accessibility vs. expression correlation (Pearson)
-2kb TSS 2kb
Highest correlation of chromatin accessibility vs. expression around TSS (Pearson)
♂PN3 ♀PN3 ♂PN5 ♀PN5 2-cell 4-cell Morula ICM TE
C
ICSI
PN3 female
PN3 male
PN5 female
PN5 male
2-cell
4-cell
Morula
ICM
TE
Chromatin accessibility
log2(TPM/10+1) ≤ 0.1
0.1 < log2(TPM/10+1) ≤ 1
1 < log2(TPM/10+1)
D
ROSI
PN3 female
PN3 male
PN5 female
PN5 male
2-cell
4-cell
Morula
ICM
TE
Chromatin accessibility
log2(TPM/10+1) ≤ 0.1
0.1 < log2(TPM/10+1) ≤ 1
1 < log2(TPM/10+1)

Figure S9. Chromatin accessibility reprogramming in ICSI and ROSI embryos.

(**A**) Heatmaps showing the scaled chromatin accessibility of stage-specific proximal NDRs in ICSI (left) and ROSI embryos (right) at the PN3 and PN5 stages. Representative GO terms and stage-specific proximal NDRs associated genes at each stage are listed on the right.

(**B**) Pearson correlation of chromatin accessibility and gene expression level around promoter regions (TSSs ± 2 kb) of all the RefSeq genes in ICSI embryos at each stage. Bar plot on the right showing the highest correlation between chromatin accessibility and gene expression level around TSS in ICSI embryos at each stage.

(**C**-**D**) Chromatin accessibility on the promoters with different expression levels in ICSI (C) and ROSI (D) embryos at each stage. The genes are divided into three groups: lowly expressed ($\log_2(TPM/10+1) \leq 0.1$), intermediately expressed ($0.1 < \log_2(TPM/1+1) \leq 1$), and highly expressed ($\log_2(TPM/10+1) > 1$).

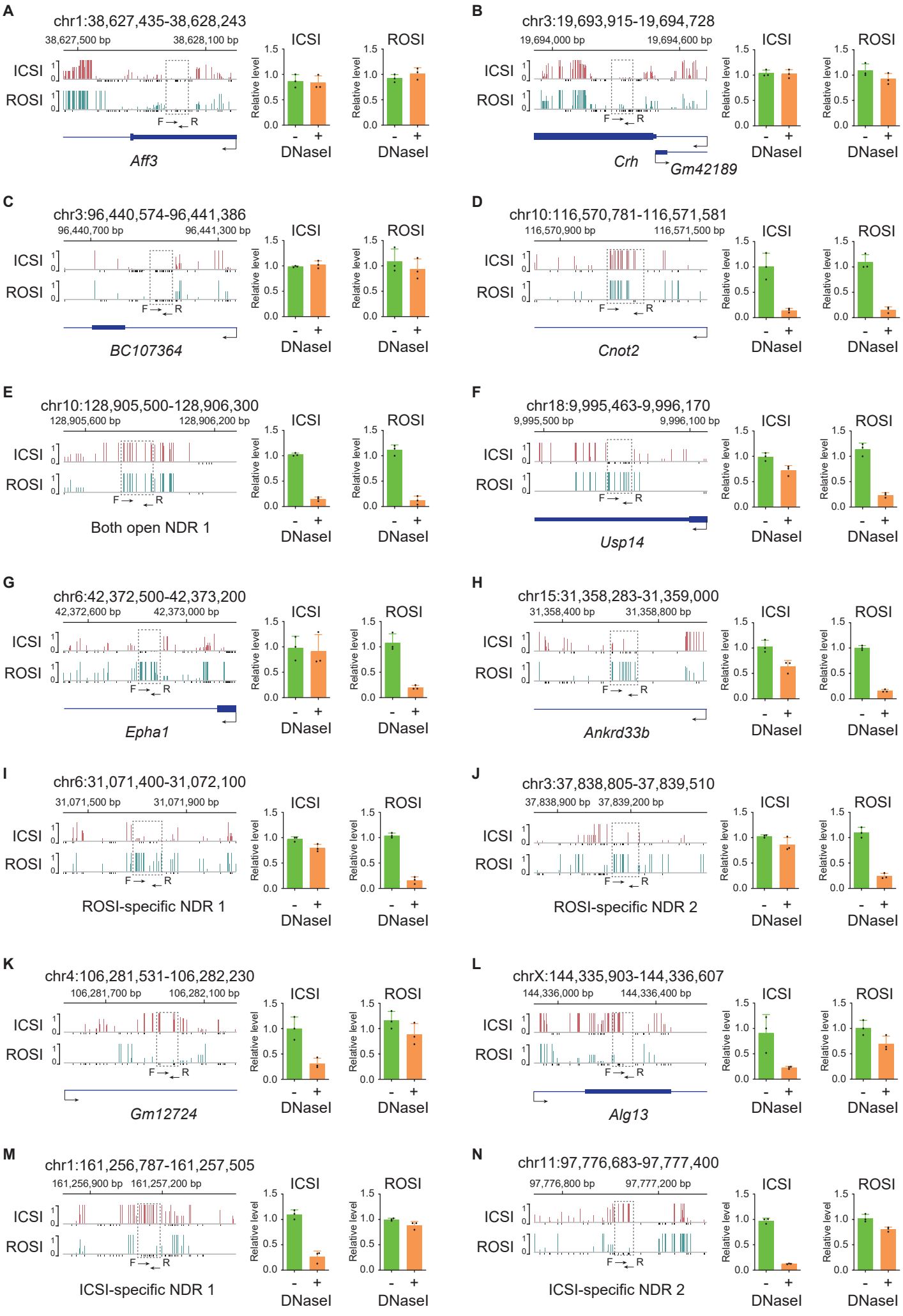
A
chr1:38,627,435-38,628,243
38,627,500 bp
38,628,100 bp
ICSI
ROSI
F
R
Aff3
ICSI
ROSI
Relative level
DNaseI
B
chr3:19,693,915-19,694,728
19,694,000 bp
19,694,600 bp
Crh
Gm42189
C
chr3:96,440,574-96,441,386
96,440,700 bp
96,441,300 bp
BC107364
D
chr10:116,570,781-116,571,581
116,570,900 bp
116,571,500 bp
Cnot2
E
chr10:128,905,500-128,906,300
128,905,600 bp
128,906,200 bp
Both open NDR 1
F
chr18:9,995,463-9,996,170
9,995,500 bp
9,996,100 bp
Usp14
G
chr6:42,372,500-42,373,200
42,372,600 bp
42,373,000 bp
Epha1
H
chr15:31,358,283-31,359,000
31,358,400 bp
31,358,800 bp
Ankrd33b
I
chr6:31,071,400-31,072,100
31,071,500 bp
31,071,900 bp
ROSI-specific NDR 1
J
chr3:37,838,805-37,839,510
37,838,900 bp
37,839,200 bp
ROSI-specific NDR 2
K
chr4:106,281,531-106,282,230
106,281,700 bp
106,282,100 bp
Gm12724
L
chrX:144,335,903-144,336,607
144,336,000 bp
144,336,400 bp
Alg13
M
chr1:161,256,787-161,257,505
161,256,900 bp
161,257,200 bp
ICSI-specific NDR 1
N
chr11:97,776,683-97,777,400
97,776,800 bp
97,777,200 bp
ICSI-specific NDR 2

Figure S10. The validation of representative loci detected as either open or closed chromatin regions in ICSI and ROSI 4-cell embryos by liDNaseI-qPCR assay.

(**A-C**) Validation of 3 representative loci (*Aff3*, *Crh*, *BC107364*) detected as both closed chromatin regions by liDNaseI-qPCR assay.

(**D-E**) Validation of 2 representative loci (*Cnot2*, both open NDR 1) detected as both open chromatin regions by liDNaseI-qPCR assay.

(**F-J**) Validation of 5 representative loci (*Usp14*, *Epha1*, *Ankrd33b*, ROSI-specific open loci1, ROSI-specific open loci2) detected as ROSI-specific open chromatin regions by liDNaseI-qPCR assay.

(**K-N**) Validation of 4 representative loci (*Gm12724*, *Alg13*, ICSI-specific open loci1, ICSI-specific open loci 2) detected as ICSI-specific open chromatin regions by liDNaseI-qPCR assay. Three biological replicates are performed for each locus above and the error bar indicates standard deviation.

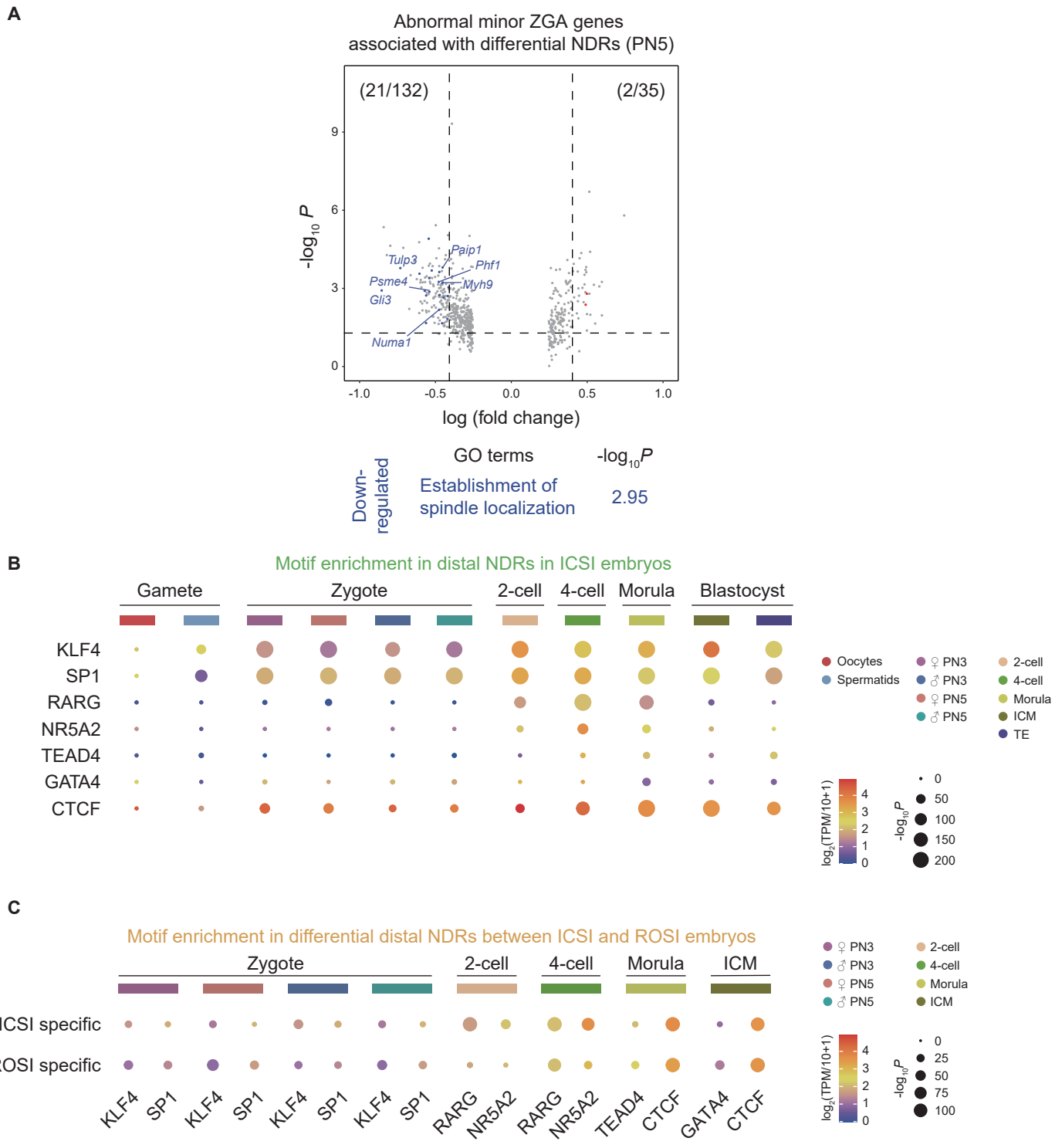
A
Abnormal minor ZGA genes
associated with differential NDRs (PN5)
(21/132)
(2/35)
-log10 P
log (fold change)
Tulp3
Paip1
Phf1
Psme4
Myh9
Gli3
Numa1
GO terms
-log10P
Down-regulated
Establishment of spindle localization
2.95
B
Motif enrichment in distal NDRs in ICSI embryos
Gamete
Zygote
2-cell
4-cell
Morula
Blastocyst
KLF4
SP1
RARG
NR5A2
TEAD4
GATA4
CTCF
Oocytes
Spermatids
♀ PN3
♂ PN3
♀ PN5
♂ PN5
2-cell
4-cell
Morula
ICM
TE
log2(TPM/10+1)
-log10P
C
Motif enrichment in differential distal NDRs between ICSI and ROSI embryos
Zygote
2-cell
4-cell
Morula
ICM
ICSI specific
ROSI specific
KLF4
SP1
RARG
NR5A2
TEAD4
CTCF
GATA4

Figure S11. The relationship between chromatin accessibility and gene expression in ROSI embryos.

(**A**) Volcano plot showing the relationship between differential gene expression of minor ZGA genes and chromatin accessibility of proximal NDRs (PN5). The blue dots represent genes whose expression levels are significantly lower in ROSI embryos and occupied with the ICSI specific-proximal NDRs (absolute GCH methylation difference > 0.1; $P < 0.05$), and the red dots are vice versa.

(**B**) Transcription factor motifs enrichment analysis of distal NDRs in ICSI embryos. Only Transcription factors expressed (TPM ≥ 10) and with motif enrichment $P < 10^{-10}$ in at least one stage are included.

(**C**) Transcription factor motifs enrichment analysis in differential distal NDRs between ROSI and ICSI embryos. Only Transcription factors expressed (TPM ≥ 10) and with motif enrichment $P < 10^{-10}$ in at least one stage are included.

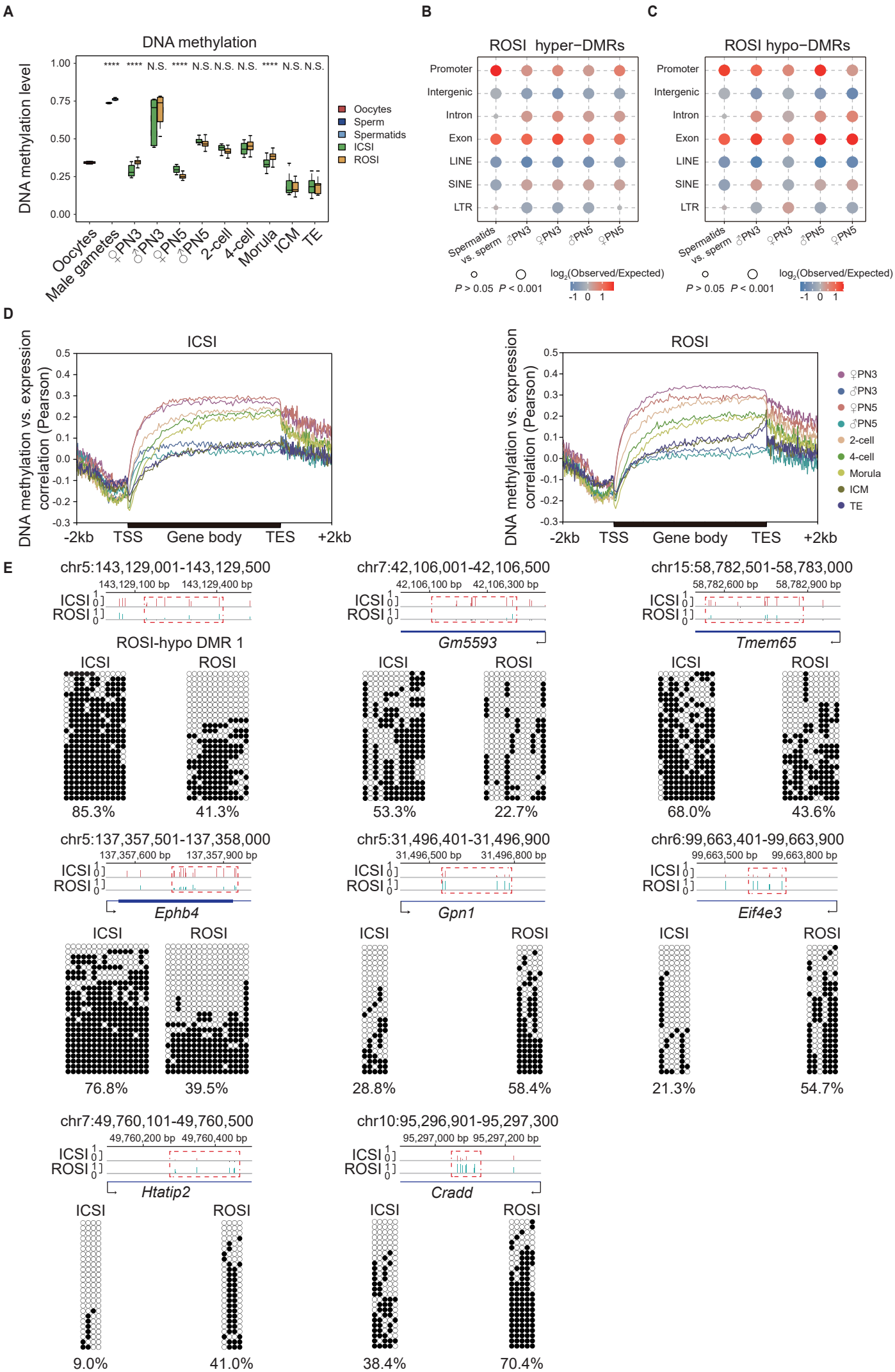
A
DNA methylation
DNA methylation level
1.00
0.75
0.50
0.25
0.00
**** **** N.S. **** N.S. N.S. N.S. **** N.S. N.S.
Oocytes
Sperm
Spermatids
ICSI
ROSI
Oocytes
Male gametes
♀PN3
♂PN3
♀PN5
♂PN5
2-cell
4-cell
Morula
ICM
TE
B
ROSI hyper−DMRs
Promoter
Intergenic
Intron
Exon
LINE
SINE
LTR
Spermatids vs. sperm
♂PN3
♀PN3
♂PN5
♀PN5
P > 0.05
P < 0.001
log2(Observed/Expected)
-1 0 1
C
ROSI hypo−DMRs
Promoter
Intergenic
Intron
Exon
LINE
SINE
LTR
Spermatids vs. sperm
♂PN3
♀PN3
♂PN5
♀PN5
P > 0.05
P < 0.001
log2(Observed/Expected)
-1 0 1
D
ICSI
DNA methylation vs. expression correlation (Pearson)
0.5
0.4
0.3
0.2
0.1
0.0
-0.1
-0.2
-0.3
-2kb
TSS
Gene body
TES
+2kb
ROSI
DNA methylation vs. expression correlation (Pearson)
0.5
0.4
0.3
0.2
0.1
0.0
-0.1
-0.2
-0.3
-2kb
TSS
Gene body
TES
+2kb
♀PN3
♂PN3
♀PN5
♂PN5
2-cell
4-cell
Morula
ICM
TE
E
chr5:143,129,001-143,129,500
143,129,100 bp
143,129,400 bp
ICSI
ROSI
ROSI-hypo DMR 1
ICSI
ROSI
85.3%
41.3%
chr7:42,106,001-42,106,500
42,106,100 bp
42,106,300 bp
ICSI
ROSI
Gm5593
ICSI
ROSI
53.3%
22.7%
chr15:58,782,501-58,783,000
58,782,600 bp
58,782,900 bp
ICSI
ROSI
Tmem65
ICSI
ROSI
68.0%
43.6%
chr5:137,357,501-137,358,000
137,357,600 bp
137,357,900 bp
ICSI
ROSI
Ephb4
ICSI
ROSI
76.8%
39.5%
chr5:31,496,401-31,496,900
31,496,500 bp
31,496,800 bp
ICSI
ROSI
Gpn1
ICSI
ROSI
28.8%
58.4%
chr6:99,663,401-99,663,900
99,663,500 bp
99,663,800 bp
ICSI
ROSI
Eif4e3
ICSI
ROSI
21.3%
54.7%
chr7:49,760,101-49,760,500
49,760,200 bp
49,760,400 bp
ICSI
ROSI
Htatip2
ICSI
ROSI
9.0%
41.0%
chr10:95,296,901-95,297,300
95,297,000 bp
95,297,200 bp
ICSI
ROSI
Cradd
ICSI
ROSI
38.4%
70.4%

Figure S12. DNA methylation reprogramming alterations from gamete to pre-implantation embryos.

(**A**) Boxplot showing the average DNA methylation levels in gametes, ROSI, and ICSI embryos. The top and bottom of the boxes indicate the first and third quartiles, while the lines inside the boxes represent the median level. ****$P < 0.0001$, N.S., not significant, unpaired two-tailed Student's *t* test.

(**B-C**) Relative enrichment analysis of hyper-DMRs (B) and hypo-DMRs (C) at different genomic regions between ROSI and ICSI embryos from gamete to zygote (PN3 and PN5 stages). The color indicates relative enrichment score. The size of circles represents the *P* value of enrichment (chi-squared test).

(**D**) Pearson correlation of DNA methylation and gene expression level along gene bodies, 2 kb upstream of TSS, and 2 kb downstream of TES of all the RefSeq genes in ICSI (left) and ROSI (right) embryos at each stage.

(**E**) 4 representative loci (ROSI-hypo DMR 1, *Gm5593*, *Tmem65*, *Ephb4*) detected as ROSI hypo-DMRs and 4 representative loci (*Gpn1*, *Eif4e3*, *Htatip2*, *Cradd*) detected as ROSI hyper-DMRs in ICSI and ROSI embryos at morula stage by bisulfite genomic PCR-based Sanger sequencing.

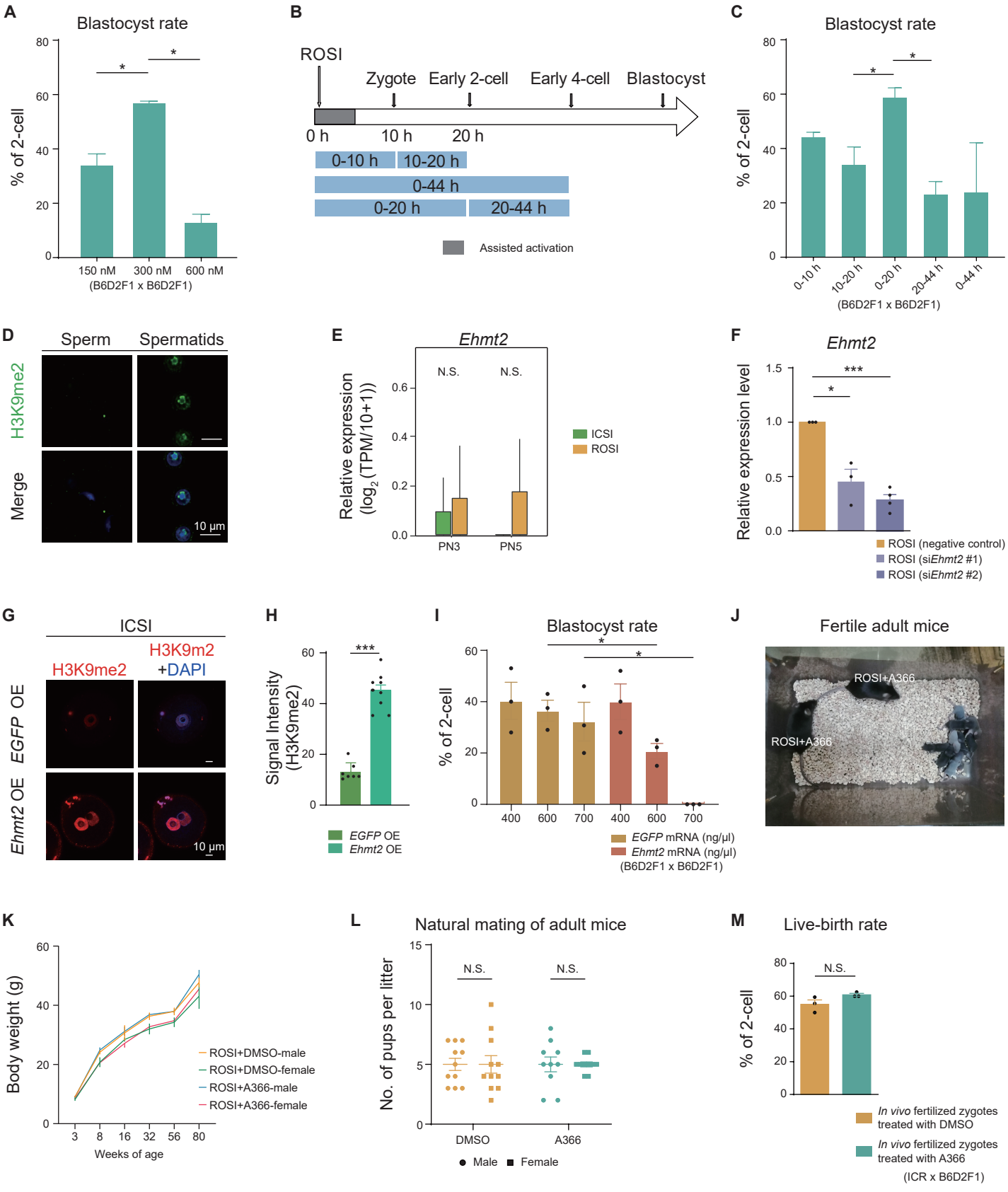
A
Blastocyst rate
% of 2-cell
150 nM
300 nM
600 nM
(B6D2F1 x B6D2F1)
B
ROSI
Zygote
Early 2-cell
Early 4-cell
Blastocyst
0 h
10 h
20 h
0-10 h
10-20 h
0-44 h
0-20 h
20-44 h
Assisted activation
C
Blastocyst rate
% of 2-cell
0-10 h
10-20 h
0-20 h
20-44 h
0-44 h
(B6D2F1 x B6D2F1)
D
Sperm
Spermatids
H3K9me2
Merge
10 μm
E
Ehmt2
Relative expression (log2 (TPM/10+1))
N.S.
N.S.
PN3
PN5
ICSI
ROSI
F
Ehmt2
Relative expression level
ROSI (negative control)
ROSI (siEhmt2 #1)
ROSI (siEhmt2 #2)
G
ICSI
H3K9me2
H3K9m2 +DAPI
EGFP OE
Ehmt2 OE
10 μm
H
Signal Intensity (H3K9me2)
EGFP OE
Ehmt2 OE
I
Blastocyst rate
% of 2-cell
EGFP mRNA (ng/μl)
Ehmt2 mRNA (ng/μl)
(B6D2F1 x B6D2F1)
J
Fertile adult mice
ROSI+A366
ROSI+A366
K
Body weight (g)
ROSI+DMSO-male
ROSI+DMSO-female
ROSI+A366-male
ROSI+A366-female
Weeks of age
L
Natural mating of adult mice
No. of pups per litter
N.S.
N.S.
DMSO
A366
Male
Female
M
Live-birth rate
% of 2-cell
N.S.
In vivo fertilized zygotes treated with DMSO
In vivo fertilized zygotes treated with A366
(ICR x B6D2F1)

Figure S13. The optimization of A366 treatment and long-term outcomes of A366-treated ROSI mice.

(**A**) Blastocyst rate of the ROSI embryos treated by A366 under different concentrations in three biological replicates. *$P < 0.05$, unpaired two-tailed Student's *t* test.

(**B**) Schematic diagram showing the time frame for A366 treatment optimization.

(**C**) Blastocyst rate of the ROSI embryos treated by A366 under different time frames in three biological replicates. *$P < 0.05$, unpaired two-tailed Student's *t* test.

(**D**) Immunofluorescence of H3K9me2 in sperm and round spermatids used in this study. Scale bars, 10 μm.

(**E**) Relative expression (log_2(TPM/10+1)) of *Ehmt2* in ROSI and ICSI embryos at the PN3 and PN5 stages, N.S., not significant, likelihood ratio test.

(**F**) Relative expression level of *Ehmt2* in ROSI embryos injected with si*Ehmt2* #1 and si*Ehmt2* #2 compared to the negative control at 22 h post-injection in three biological replicates. *$P < 0.05$, ***$P < 0.001$, unpaired two-tailed Student's *t* test.

(**G**) Immunofluorescence of H3K9me2 in ICSI embryos (PN5) that overexpressed *Ehmt2*. Scale bars, 10 μm.

(**H**) Bar graph showing the fluorescence intensity of H3K9me2 in ICSI embryos (PN5) that overexpressed *Ehmt2* (n = 9) and *EGFP* (n = 7) in three biological replicates. ***$P < 0.001$, unpaired two-tailed Student's *t* test.

(**I**) Blastocyst rate of ROSI embryos injected with *Ehmt2* mRNA under different concentrations in three biological replicates. *$P < 0.05$, unpaired two-tailed Student's *t* test.

(**J**) Representative adult mice from A366-treated ROSI embryos and their pups.

(**K**) Line chart showing the body weight of mice (from 3 to 80 week) from ROSI group treated by A366 and the untreated control. n = 3 per group.

(**L**) Dot plot showing the litter size of natural mating adult mice from ROSI group treated by A366 (n = 10) and the untreated control (n = 11) in three biological replicates. N.S., not significant, unpaired two-tailed Student's *t* test.

(**M**) Live-birth rate of *in vivo* fertilized zygotes treated by A366 and the untreated control (DMSO) in three biological replicates. N.S., not significant, unpaired two-tailed Student's *t* test.

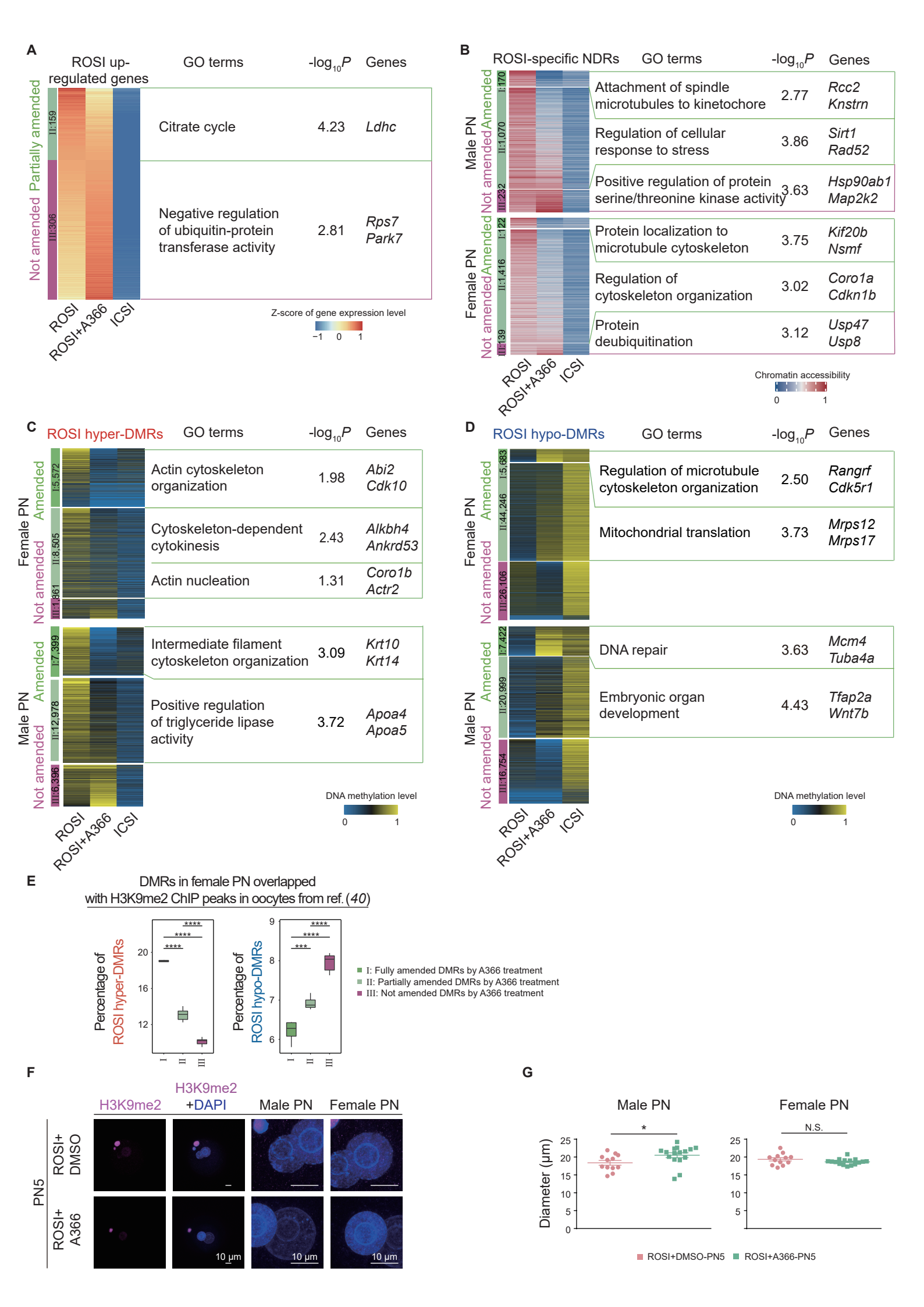
A
ROSI up-regulated genes
GO terms
-log10P
Genes
Partially amended
Not amended
II:159
III:306
Citrate cycle
4.23
Ldhc
Negative regulation of ubiquitin-protein transferase activity
2.81
Rps7
Park7
ROSI
ROSI+A366
ICSI
Z-score of gene expression level
−1 0 1
B
ROSI-specific NDRs
GO terms
-log10P
Genes
Male PN
Amended
Not amended
I:170
II:1,070
III:232
Attachment of spindle microtubules to kinetochore
2.77
Rcc2
Knstrn
Regulation of cellular response to stress
3.86
Sirt1
Rad52
Positive regulation of protein serine/threonine kinase activity
3.63
Hsp90ab1
Map2k2
Female PN
Amended
Not amended
I:122
II:1,416
III:139
Protein localization to microtubule cytoskeleton
3.75
Kif20b
Nsmf
Regulation of cytoskeleton organization
3.02
Coro1a
Cdkn1b
Protein deubiquitination
3.12
Usp47
Usp8
ROSI
ROSI+A366
ICSI
Chromatin accessibility
0 1
C
ROSI hyper-DMRs
GO terms
-log10P
Genes
Female PN
Amended
Not amended
I:5,572
II:8,505
III:1,861
Actin cytoskeleton organization
1.98
Abi2
Cdk10
Cytoskeleton-dependent cytokinesis
2.43
Alkbh4
Ankrd53
Actin nucleation
1.31
Coro1b
Actr2
Male PN
Amended
Not amended
I:7,399
II:12,978
III:6,396
Intermediate filament cytoskeleton organization
3.09
Krt10
Krt14
Positive regulation of triglyceride lipase activity
3.72
Apoa4
Apoa5
ROSI
ROSI+A366
ICSI
DNA methylation level
0 1
D
ROSI hypo-DMRs
GO terms
-log10P
Genes
Female PN
Amended
Not amended
I:5,683
II:44,246
III:26,106
Regulation of microtubule cytoskeleton organization
2.50
Rangrf
Cdk5r1
Mitochondrial translation
3.73
Mrps12
Mrps17
Male PN
Amended
Not amended
I:7,422
II:20,999
III:16,754
DNA repair
3.63
Mcm4
Tuba4a
Embryonic organ development
4.43
Tfap2a
Wnt7b
ROSI
ROSI+A366
ICSI
DNA methylation level
0 1
E
DMRs in female PN overlapped with H3K9me2 ChIP peaks in oocytes from ref. (40)
Percentage of ROSI hyper-DMRs
Percentage of ROSI hypo-DMRs
****
***
I
II
III
I: Fully amended DMRs by A366 treatment
II: Partially amended DMRs by A366 treatment
III: Not amended DMRs by A366 treatment
F
H3K9me2
H3K9me2 +DAPI
Male PN
Female PN
PN5
ROSI+ DMSO
ROSI+ A366
10 μm
G
Male PN
Female PN
*
N.S.
Diameter (μm)
ROSI+DMSO-PN5
ROSI+A366-PN5

Figure S14. The amending of gene expression, chromatin accessibility, and DNA methylation in ROSI embryos by A366 treatment.

(**A**) Heatmap showing the expression alterations of ROSI up-regulated genes at the PN5 stage after A366 treatment. I: gene expression fully amended by A366; II: gene expression partially amended by A366; III: gene expression not amended by A366. The number of genes in each category is shown on the left. Representative GO terms and genes in each category are shown on the right.

(**B**) Heatmaps showing the chromatin accessibility alterations of ROSI-specific NDRs at the PN5 stage after A366 treatment. I: chromatin accessibility fully amended by A366; II: chromatin accessibility partially amended by A366; III: chromatin accessibility not amended by A366. The number of NDRs in each category is shown on the left. Representative GO terms and genes in each category are shown on the right.

(**C-D**) Heatmaps showing the DNA methylation alterations of ROSI hyper-DMRs (C) and hypo-DMRs (D) at the PN5 stage after A366 treatment. I: DNA methylation fully amended by A366; II: DNA methylation partially amended by A366; III: DNA methylation not amended by A366. The number of DMRs in each category is shown on the left. Representative GO terms and genes in each category are shown on the right.

(**E**) Boxplots showing the percentage of overlapping between randomly selected DMRs within each category (fig. S14, C and D) and H3K9me2 ChIP peaks from ref. (*40*). One third of DMRs in each category are randomly selected independently to calculate the overlapping percentage and are repeated for 10 times to estimate the significance of difference. ***$P < 0.001$, ****$P < 0.0001$, unpaired two-tailed Student's *t* test.

(**F**) Immunofluorescence of H3K9me2 in A366-treated ROSI embryos and the untreated control (PN5). Embryos are fixed and permeabilized using 4% paraformaldehyde containing 0.2% Triton X-100 for 20 min at room temperature. The magnified image of male and female pronuclei are shown on the right. Scale bars, 10 μm.

(**G**) Dot plots showing the diameter of male (left) and female (right) pronuclei in A366-treated ROSI embryos (n = 14) and the untreated control (n = 14) (PN5) in three biological replicates. *$P < 0.05$, N.S., not significant, unpaired two-tailed Student's *t* test.